Tellus
SERIES B
CHEMICAL
AND PHYSICAL
METEOROLOGY
PUBLISHED BY THE INTERNATIONAL METEOROLOGICAL INSTITUTE IN STOCKHOLM

Tellus (2008), 60B, 771–781
Printed in Singapore. All rights reserved

TELLUS

Climatic significance of tree-ring width and $\delta^{13}C$ in a Spanish pine forest network

By LAIA ANDREU[1,2]*, OCTAVI PLANELLS[1], EMILIA GUTIÉRREZ[1], GERHARD HELLE[2] and GERHARD H. SCHLESER[3], [1]*Departament d'Ecologia, Universitat de Barcelona, Av. Diagonal 645, 08028 Barcelona, Spain;* [2]*Institut für Chemie und Dynamik der Geosphäre, Institut 5: Sedimentäre Systeme, Forschungszentrum Jülich GmbH, Leo-Brandt Strasse, 52425 Jülich, Germany;* [3]*GeoForschungszentrum Potsdam, Sektion 3.3: Klimadynamik und Sedimente, Telegrafenberg 14473 Potsdam, Germany*

(Manuscript received 31 July 2007; in final form 6 June 2008)

ABSTRACT

This paper examines tree-ring width and $\delta^{13}C$ chronologies from a network of five Iberian pine forests to determine their sensitivity to climate variability under different site conditions. Interseries comparisons revealed better and more homogenous agreement among $\delta^{13}C$ records than among tree-ring width series of the different sites. This suggests that $\delta^{13}C$ ratios may preferentially record large-scale climatic signals, whereas ring-width variations may reflect more local factors. A negative relationship was found between ring-width and $\delta^{13}C$. As inferred from response function analyses, ring-width and $\delta^{13}C$ showed significant relationships with climate. The analyses of different sites and species revealed unshared tree-ring width responses to summer temperature and precipitation, whereas all $\delta^{13}C$ series were highly sensitive to current year summer precipitation and, to a lesser extent, to current summer temperature. A strong summer precipitation signal seems to dominate the $\delta^{13}C$ of trees growing under Mediterranean climate, even when the mean climatic site conditions do not indicate distinct summer drought. Therefore, $\delta^{13}C$ values reflect precipitation variability during the summer season better than tree-ring widths. This demonstrates that $\delta^{13}C$ from tree-rings can be a very useful tool for climatic reconstruction in the Mediterranean region, especially when climate-growth relationships are weak.

1. Introduction

Tree-rings are a valuable source of long-term information about environmental change. As tree growth is affected by climate variation, past climate is frequently reconstructed from changes in annual ring-widths or wood density. However, the $^{13}C/^{12}C$ ratio of tree-ring cellulose is also a useful proxy to assess past climate variability (e.g. Hemming et al., 1998; McCarroll and Pawellek, 2001; Helle et al., 2002; Helle and Schleser, 2004), soil water content (e.g. Panek and Goldstein, 2001), water-use efficiency (e.g. Matzner et al., 2001; Ponton et al., 2001) or hydraulic properties of the water-conducting system of stems and branches (Panek, 1996). Until recently, there have been few studies comparing and combining environmental information from $\delta^{13}C$ of tree-ring cellulose and ring-widths (Robertson et al., 1997a,b; Gagen et al., 2004, 2006).

Mean annual temperature over Europe increased by about 0.8 °C during the 20th century. Larger warming was observed over the Iberian Peninsula (IPCC, 2001), where the 1980–95 period was characterized by intense droughts, producing serious damage to several woody species (Peñuelas et al., 2001). Changes in the variability of tree growth to changing climatic conditions among conifer forests have been previously reported in Spain (e.g. Tardif et al., 2003; Macias et al., 2006; Andreu et al., 2007). However, dendroclimatological studies using stable isotopes are particularly rare from the Iberian Peninsula (Ferrio et al., 2003; Ferrio and Voltas, 2005). In the literature, low-frequency variations in $\delta^{13}C$ of tree-ring series from the late 19th and 20th century have been generally linked with physiological responses to increasing atmospheric CO_2 concentrations, in conjunction with declining in $\delta^{13}C$ values of atmospheric CO_2 (e.g. Feng, 1998), whereas high frequency fluctuations in $\delta^{13}C$ have been related to climatic variables (Feng and Epstein, 1995; Hemming et al., 1998; Tang et al., 1999). Here, we present chronologies of tree-ring width and $\delta^{13}C$ from a network of Spanish forests for the last two centuries. We investigated the particular value of carbon isotope analysis by assessing the nature and strength of the climatic signal recorded in ring-width and $\delta^{13}C$ chronologies.

Our study was carried out on the Iberian Peninsula with three pine species located at the edge of their phytogeographical distribution area: *Pinus sylvestris* L., *P. uncinata* Ramond ex.

*Corresponding author.
e-mail: laiandreu@ub.edu
DOI: 10.1111/j.1600-0889.2008.00370.x

DC and *P. nigra* Arnold subsp. *salzmannii*. The first two species are of Eurosiberian origin and grow at the southern and western limit of their distribution. The latter, a typical Mediterranean pine species, grows at its western boundary (Blanco et al., 1997). The selected sites were chosen because tree species show a particular susceptibility to climatic variations, modified by site ecology, at the boundary of their geographical distribution (Fritts, 1976).

The sites are located quite far from each other and are characterized by different atmospheric circulation patterns and related precipitation regimes: Atlantic, continental and Mediterranean. Hence, different responses of ring-width and δ^{13}C were expected between the sites and species. Species-dependent responses were addressed by studying different species (*P. sylvestris* and *P. uncinata*) from two nearby forest stands of the Urbión range.

Considering current climatic conditions and previous studies on tree-ring width series (Tardif et al., 2003; Macias et al., 2006; Andreu et al., 2007), we wanted to evaluate the common macroclimatic signal shared by the δ^{13}C and ring-width series of a network of forests. Specifically, the aims of this investigation were: (1) to compare ring-width and δ^{13}C chronologies from different pine species of five forests, growing under different climatic influences, and (2) to assess the nature and strength of climatic signals recorded in the tree-ring width and δ^{13}C series.

2. Material and methods

Five forest stands were sampled on the Iberian Peninsula (Fig. 1). One *Pinus nigra* stand located in the southeast (*pn*Caz), two *P. sylvestris* forests in the north and the northwest (*ps*Urb and *ps*Lil, respectively), and two *P. uncinata* forests in the north and northeast (*pu*Urb and *pu*Ped, respectively). *Ps*Urb and *pu*Urb are located only 10 km away from each other, allowing for assessment of species-specific responses to similar climatic conditions. Sampling focused on the oldest natural forest stands in the area. Site characteristics are described in Table 1. At each site, more than fifteen trees were cored with an increment borer at around 1.30 m stem height. At least four cores were taken from each tree: two for building ring-width chronologies and two for isotope analyses.

2.1. Ring-width chronologies

Cores were sanded until wood cells were clearly visible under the microscope (Stokes and Smiley, 1968). All samples were visually cross-dated following the procedures described by Yamaguchi (1991) to avoid miscounting by missing (locally absent) or false (multiple) rings. After cross-dating, the ring-widths were measured with an accuracy of 0.01 mm using an ANIOL semi-automatic device (Aniol, 1983). The resulting series underwent a cross-dating quality control, using the statistical program COFECHA (Holmes, 1983).

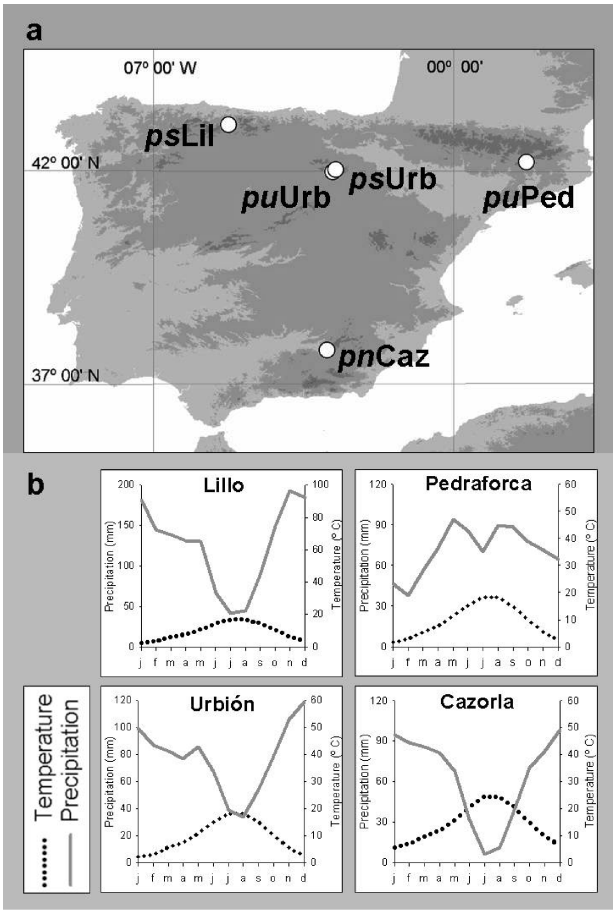

Fig. 1. Geographical locations of the study sites in the Iberian Peninsula (a) and ombrotermic climate diagrams of each region (b).

Individual ring-width series were standardized to make them comparable (Fritts, 1976). Standardization was accomplished using the program TURBOARSTAN, the windows version of ARSTAN (Cook, 1985). First a power transformation of raw series was applied to stabilize variance (Cook and Peters, 1997; Helama et al., 2004). Second, the series were detrended by negative exponential or linear fitting. These conservative methods were applied to remove age-related trends. Third, an autoregressive model was applied to remove autocorrelation, resulting in white-noise indices series. A robust mean, which reduces variance and bias caused by extreme values, was computed at the end of each step (Cook and Briffa, 1990). In this way, standard chronologies 'std_c' (detrended; Fig. 2), and residual chronologies 'res_c' (detrended without autocorrelation) were obtained. The reliable time span of the chronologies was determined by the Expressed Population Signal criteria (EPS > 0.85, Wigley et al., 1984). Descriptive statistics calculated using COFECHA and ARSTAN software are presented to allow comparisons among sites (Table 2). All the chronologies had an EPS exceeding the commonly accepted minimum value of 0.85, except for *ps*Urb std_c, which showed a slightly lower value.

Table 1. Characteristics of the study sites.

Site	Species	Site code	Range	Latitude	Longitude	Altitude (m a.s.l.)	Aspect	Slope	Stand density
Cazorla	*Pinus nigra*	*pn*Caz	Betic	37°48′ N	02°57′ W	1800	SW	15°	Open forest
Pinar de Lillo	*Pinus sylvestris*	*ps*Lil	Cantabrian	43°03′ N	05°15′ W	1600	NW	28°	Mainly open forest
Pedraforca	*Pinus uncinata*	*pu*Ped	Pre-Pyrenees	42°14′ N	01°42′ E	2100	NE	36°	Open forest
Urbión	*Pinus sylvestris*	*ps*Urb	Iberian	42°00′ N	02°49′ W	1750	NE	23°	Closed forest
Urbión	*Pinus uncinata*	*pu*Urb	Iberian	41°58′ N	02°45′ W	1950	SW	10°	Closed forest

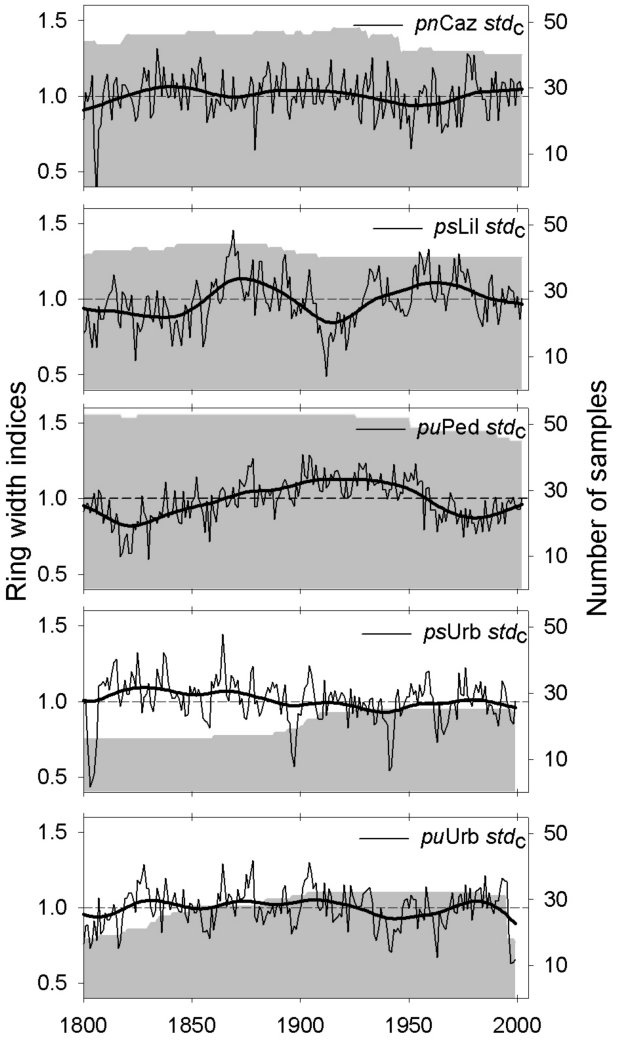

Fig. 2. Standard ring-width chronologies '*std*$_c$' (black lines). Fifty-year smoothing splines fitted on *std*$_c$ (thick grey lines) are depicted to show long-term fluctuations. Sample depths are shown as grey areas (right axis).

2.2. Isotope chronologies

For *pn*Caz, *ps*Lil and *pu*Ped, eight cross-dated samples from four different trees were selected (at least two cores per tree), whereas for *ps*Urb and *pu*Urb, eight trees were selected (one core per tree; Table 3). For each site, tree-rings were separated and pooled year by year (Leavitt and Long, 1984; Treydte et al., 2001). α-cellulose was extracted to avoid isotope variations due to varying compositions of wood components such as lignin (Wilson and Grinsted, 1977) or resins, which show a systematically different isotopic signature. The extraction of cellulose employed acetic acid, sodium chlorite and sodium hydroxide (Sohn and Reiff, 1942; Loader et al., 1997). The α-cellulose was homogenized in two different ways: *ps*Urb and *pu*Urb samples were ground with an ultra centrifugation mill (Retsch ZM1, mesh size of 0.5 mm), whereas samples from *pn*Caz, *ps*Lil and *pu*Ped were homogenized with an ultrasonic device developed at the Forschungszentrum Jülich GmbH, Germany, providing a higher sample throughput. Carbon isotopes were measured by combusting α-cellulose to CO_2 in an elemental analyser (Fisons NA 1500 NC) coupled via an open split to an isotope ratio mass spectrometer (Micromass Optima) operated in continuous flow mode. The precision was generally better than 0.1‰. The isotope signature expressed as δ^{13}C is given in the delta notation, relative to the standard V-PDB (IAEA, 1995):

$$\delta^{13}C_{\text{sample}} = \left[\frac{(^{13}C/^{12}C)_{\text{sample}}}{(^{13}C/^{12}C)_{\text{V-PDB}}} - 1\right] \times 1000 \quad \text{in per mil}(‰) \tag{1}$$

All δ^{13}C chronologies (raw data) show a decreasing trend attributed to the rise of ^{13}C-depleted atmospheric CO_2 due to fossil fuel burning and deforestation since industrialization (Fig. 3). The main goal of this study was to assess the climatic signal of these series. Hence, this non-climatic trend related to changes in atmospheric δ^{13}C was removed from the raw δ^{13}C chronologies. To obtain the corrected δ^{13}C chronologies ($\delta^{13}C_c$), we subtracted for each year the annual changes in δ^{13}C of atmospheric CO_2, obtained from ice cores and direct measurements (Leuenberger, 2007). Similar to dendrochronological procedures, an autoregressive (AR) model was applied using the program FMT from the DPL software (Holmes, 1992) resulting in autocorrelation-free tree-ring δ^{13}C chronologies ($\delta^{13}C.AR_c$). Table 3 shows the main statistics of the raw data, as well as $\delta^{13}C_c$ and $\delta^{13}C.AR_c$ data.

2.3. Comparison among sites and proxies

To assess the interseries relationships, Pearson correlation coefficients were calculated for the 20th century (1901–1999)

Table 2. Mean correlation of the tree ring-width chronologies calculated using COFECHA software for the period 1800–2002.

				std_c		res_c		EPS (1901–1999)		
Site ID	Time-span	Trees/radii	Mean correlation	MS_x	AC1	MS_x	AC1	Tree/radii	std_c	res_c
*pn*Caz	1800–2002	29/53	0.682	0.14	0.60	0.16	0.00	24/36	0.925	0.957
*ps*Lil	1800–2002	21/44	0.594	0.11	0.69	0.13	0.03	19/40	0.876	0.89
*pu*Ped	1800–2003	21/53	0.591	0.08	0.67	0.10	−0.01	19/45	0.902	0.906
*ps*Urb	1800–1999	15/25	0.579	0.09	0.73	0.11	0.07	12/20	0.764	0.854
*pu*Urb	1800–1999	17/32	0.571	0.09	0.64	0.11	0.01	9/16	0.844	0.878

Note: Mean Sensitivity (MS_x), a measure of the inter-annual variability, first-order autocorrelation (AC1) for std_c and res_c and the Expressed Population Signal statistic (EPS) were calculated for the period 1901–1999, using the ARSTAN software.

Table 3. Statistics of raw, corrected ($\delta^{13}C_c$) and without autocorrelation ($\delta^{13}C.AR_c$) $\delta^{13}C$ tree-ring chronologies.

			Raw $\delta^{13}C$ (‰)					$\delta^{13}C_c$ (‰)					$\delta^{13}C.AR_c$ (‰)	
Site ID	Time-span	Trees/ Cores	Mean ± SD	Min	Max	Range	PAC1	Mean ± SD	Min	Max	Range	PAC1	Mean ± SD	PAC1
*pn*Caz	1800–2002	4/9	−21.38 ± 0.62	−22.9	−20.4	2.46	0.81	−20.95 ± 0.35	−22.0	−20.2	1.75	0.43	0.98 ± 0.32	0.06
*ps*Lil	1800–2002	4/10	−22.53 ± 0.63	−24.2	−21.1	3.05	0.51	−22.11 ± 0.52	−23.5	−21.0	2.46	0.32	0.92 ± 0.49	−0.05
*pu*Ped	1800–2002	4/8	−22.35 ± 0.56	−24.3	−21.0	3.32	0.47	−21.93 ± 0.45	−23.2	−20.6	2.64	0.15	0.94 ± 0.45	−0.13
*ps*Urb	1900–1999	8/8	−23.55 ± 0.58	−24.9	−22.5	2.36	0.66	−22.86 ± 0.37	−24.0	−21.9	2.05	0.21	1 ± 0.36	0.01
*pu*Urb	1800–1999	8/8	−21.91 ± 0.82	−24.5	−20.3	4.27	0.83	−21.5 ± 0.5	−23.0	−20.2	2.85	0.57	1 ± 0.39	−0.02

Minimum (Min); Maximum (Max); First order partial autocorrelation (PAC1).

among the ring-width chronologies (std_c and res_c) and the corrected $\delta^{13}C$ chronologies ($\delta^{13}C_c$ and $\delta^{13}C.AR_c$). The analysed period represents the common time span among the chronologies, due to the shorter length of the *ps*Urb $\delta^{13}C$ chronology that started in 1900. Moreover, four Principal Component Analyses (PCAs) were computed to evaluate the shared variance among the different chronologies (std_c.PCA, res_c.PCA, $\delta^{13}C_c$.PCA, $\delta^{13}C.AR_c$.PCA). Additionally, to define the relationship between both proxies, two PCAs were computed among the series with autocorrelation (std_c-$\delta^{13}C_c$.PCA) and without autocorrelation (res_c-$\delta^{13}C.AR_c$.PCA).

2.4. Climate relationships

Pearson correlation and response function analyses were performed using the program DENDROCLIM2002 (Biondi and Waikul, 2004) to quantify the climate-growth and the climate-$\delta^{13}C$ relationships. Response functions (Fritts, 1976) were used to avoid the problem of multi colinearity, i.e. interdependence commonly found in multi-variable sets of meteorological data. The tree-ring records were expressed as functions of a set of meteorological data (predictors), computing stepwise multiple regressions after the orthogonalization of the predictors by PCAs. Thus, response function coefficients are multivariate estimates from a principal component regression model. The significance of the calculated Pearson correlation coefficients, as well as the response function partial regression coefficients was computed based on 1000 bootstrapped iterations, obtained by random extraction with replacement from the initial data set (Guiot, 1991). The use of bootstrap techniques allowed the estimation of 95% probability confidence intervals by means of a virtual increase of sample size. The analysed period of tree growth was from July of the previous to October of the current year.

The meteorological data used in this study correspond to mean monthly temperature and total precipitation from 1931 to 2003. These data belong to a Spanish gridded data set (25 × 25 km grid-box) created by the Instituto Nacional de Meteorologia (INM). The nearest grid-box data were selected for each site, choosing the same set for *ps*Urb and *pu*Urb due to their proximity.

3. Results

3.1. Relationship among chronologies

Table 4 shows Pearson correlation coefficients among std_c and $\delta^{13}C_c$ for the 20th century. Few significant relationships were found among std_c, except for the highly significant correlation between *ps*Urb and *pu*Urb ($r = 0.669$; $p < 0.01$), the two sites located close to each other. This was the only case where std_c reached higher values than the corresponding $\delta^{13}C_c$. All the other correlations among $\delta^{13}C_c$ were higher and significant. The correlation between *ps*Lil and *pu*Urb turned out to be an

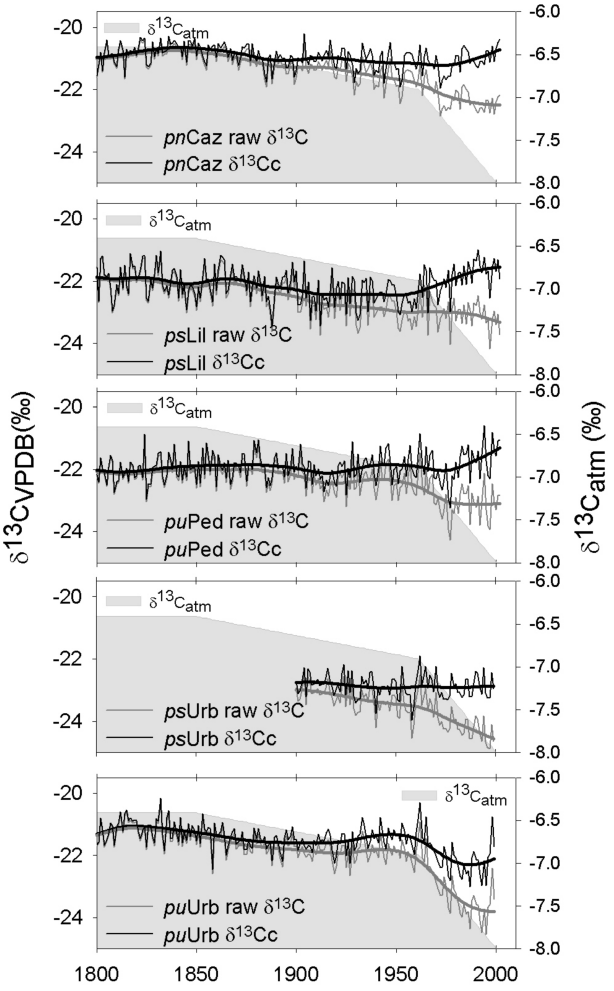

Fig. 3. Raw δ^{13}C chronologies (grey lines) and corrected δ^{13}C chronologies "$\delta^{13}C_c$" (black lines), see methodology for details, Fifty-year smoothing splines fitted on the raw δ^{13}C chronologies (thick grey lines) and $\delta^{13}C_c$ (thick black lines) are depicted to show long-term fluctuations. The $\delta^{13}C_{atm}$ decrease according to Leuenberger 2007 is indicated shown by the grey area (right axis).

unusual case because it showed non-significant values between std_c and significant negative coefficients between $\delta^{13}C_c$. The $\delta^{13}C_c$ mean correlation (0.268 ± 0.18) was higher than the std_c (0.156 ± 0.22).

All Pearson correlation coefficients were higher among $\delta^{13}C.AR_c$ than among res_c (Table 5), except for two cases. As above, correlation between *ps*Urb and *pu*Urb was higher for res_c than for $\delta^{13}C.AR_c$. The same was found between *ps*Lil and *pu*Urb. A higher mean correlation with a smaller standard deviation (SD) was also found for $\delta^{13}C.AR_c$ (0.367 ± 0.08) in comparison with res_c (0.324 ± 0.17).

Table 6 shows that the first and the second principal components (PC1 and PC2, respectively) were significant in std_c.PCA, res_c.PCA and $\delta^{13}C_c$.PCA, whereas only PC1 was significant in $\delta^{13}C.AR_c$.PCA. On one hand, the highest explained variance was attained by $\delta^{13}C.AR_c$.PC1 (49.4%) followed by res_c.PC1 (47.5%), indicating the highest sensitivity to a common climate signal of these types of chronologies.

On the other hand, std_c-$\delta^{13}C_c$.PCA and res_c-$\delta^{13}C.AR_c$.PCA showed four and three significant PCs, respectively. Figure 4 illustrates the relationships between both kinds of parameters depicting the scatter plot of the PC1 and PC2 loadings. The PC1 shows positive and negative loadings for std_c and $\delta^{13}C_c$, respectively (Fig. 4a). Similarly, res_c and $\delta^{13}C.AR_c$ also show positive and negative loadings with PC1 (Fig. 4b). There is a clear segregation of the two types of chronologies (width and δ^{13}C) along the PC1s, which explains about the 30% of the variance. Pearson correlations between both proxies at each site (Table 7) confirm the negative relationship: all correlations were negative except one, most being low and not significant. Despite the significance of other PCs, we focused on PC1, the maximum percentage of common variance shared by all the involved chronologies because shared growth variability can be interpreted as a common response to regional climate.

Removal of autocorrelation from the tree-ring series resulted in higher correlation coefficients. All correlations were higher among res_c (Table 5) than among std_c (Table 4), raising the mean correlation from 0.156 (std_c) to 0.324 (res_c). The std_c.PC1 explained lower variance than the res_c.PC1 (Table 6). Generally, correlation coefficients among $\delta^{13}C_c$ (Table 4) also increased after autocorrelation removal (Table 5). The mean correlation increased from 0.268 ($\delta^{13}C_c$) to 0.367 ($\delta^{13}C.AR_c$). However, changes in the correlation coefficients between $\delta^{13}C_c$ and $\delta^{13}C.AR_c$ after removal of autocorrelation were found to be smaller than between std_c and res_c. The $\delta^{13}C_c$.PC1 explained less variance than the $\delta^{13}C.AR_c$.PC1 (Table 6).

3.2. Climate relationships

Significant correlation and response function partial regression (RF) coefficients were found between both tree-ring proxies and climate. For each site, similar but not identical, responses were found for std_c and res_c, as well as for $\delta^{13}C_c$ and $\delta^{13}C.AR_c$ (results not shown). However, no distinct pattern was found among sites regarding which series, with (std_c/$\delta^{13}C_c$) or without autocorrelation (res_c/$\delta^{13}C.AR_c$), showed the highest correlation with meteorological data. For example, at the *pn*Caz site, res_c and $\delta^{13}C_c$ achieved the highest values versus temperature and precipitation, whereas at the *ps*Lil site, a more heterogeneous picture emerged. In the latter case, the highest correlations with temperature were found with std_c and $\delta^{13}C_c$, but the highest correlations with precipitation were found using res_c and $\delta^{13}C.AR_c$. *Pu*Ped, *ps*Urb and *pu*Urb also revealed mixed behaviour, depending on the standardization method and the meteorological variables chosen.

Table 4. Pearson correlation coefficients among std_c and $\delta^{13}C_c$ of different sites from 1901 to 1999.

std_c mean ± SD	$\delta^{13}C_c$ mean ± SD	*pn* Caz		*ps* Lil		*pu* Ped		*ps* Urb		*pu* Urb	
0.156 ± 0.22	**0.268** ± 0.18	std_c	$\delta^{13}C_c$	std_c	$\delta^{13}C_c$	std_c	$\delta^{13}C_c$	std_c	$\delta^{13}C_c$	std_c	$\delta^{13}C_c$
pn Caz		1	1	0.038	**0.250***	−0.022	**0.325****	0.244*	**0.346****	0.218*	**0.223***
ps Lil				1	1	−0.126	**0.364****	0.200*	**0.374****	0.013	**−0.204***
pu Ped						1	1	0.141	**0.360****	0.189	**0.255***
ps Urb								1	1	**0.670****	0.384**
pu Urb										1	1

Numbers in bold indicate the highest or more significant coefficients between each pair of correlations.
$^*p < 0.05$; $^{**}p < 0.01$.

Table 5. Pearson correlation coefficients among res_c and $\delta^{13}C.AR_c$ of different sites from 1901 to 1999.

res_c mean ± SD	$\delta^{13}C.AR_c$ mean ± SD	*pn* Caz		*ps* Lil		*pu* Ped		*ps* Urb		*pu* Urb	
0.324 ± 0.17	**0.367** ± 0.08	std_c	$\delta^{13}C_c$	std_c	$\delta^{13}C_c$	std_c	$\delta^{13}C_c$	std_c	$\delta^{13}C_c$	std_c	$\delta^{13}C_c$
pn Caz		1	1	0.275**	**0.310****	0.019	**0.309****	0.296**	**0.321****	0.227*	**0.303****
ps Lil				1	1	0.197	**0.349****	0.387**	**0.456****	**0.348****	0.251*
pu Ped						1	1	0.365**	**0.439****	0.439**	**0.465****
ps Urb								1	1	**0.682****	0.466**
pu Urb										1	1

Numbers in bold indicates the highest coefficients between each pair of correlations.
$^*p < 0.05$; $^{**}p < 0.01$.

Table 6. Number of chronologies involved in each PCA performed among chronologies and the variance explained (%) by each significant PC from 1901 to 1999.

PCAs	N° chronologies	PC1	PC2	PC3	PC4
std_c	5	37.4	23.1	ns	ns
res_c	5	47.5	20.6	ns	ns
$\delta^{13}C_c$	5	42.5	24.2	ns	ns
$\delta^{13}C.AR_c$	5	49.4	ns	ns	ns
std_c-$\delta^{13}C_c$	10	25.3	17.7	16.9	10.0
res_c-$\delta^{13}C.AR_c$	10	29.3	21.1	10.1	ns

ns = non significant

To assess the nature and strength of the climatic signal recorded in width and $\delta^{13}C$ tree-ring chronologies, considering similar frequency domain, we can either use res_c and $\delta^{13}C.AR_c$ (annual frequency) or std_c and $\delta^{13}C_c$ (annual and lower frequencies). Although removing autocorrelation did not result in a clearer climatic signal for all the chronologies, res_c versus $\delta^{13}C.AR_c$ were chosen for further detailed exploration because all the residual chronologies (res_c) achieved a reliable EPS for the studied period (Table 2), and the variance explained by the PC1 was higher (Table 6).

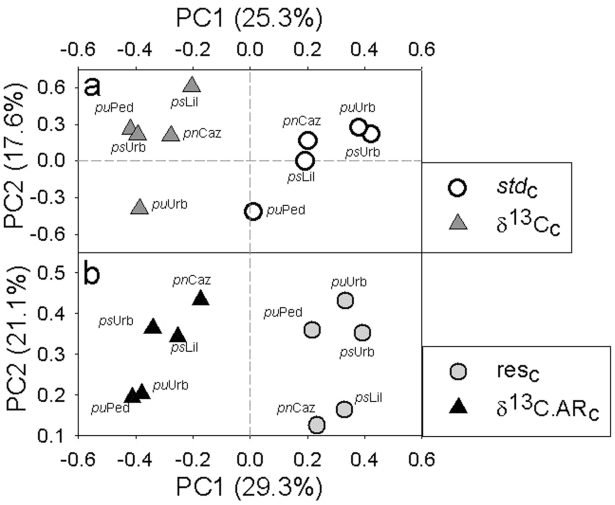

Fig. 4. Scatter plot of PC1 and PC2 loadings of the PCA performed for the width and $\delta^{13}C$ tree-ring chronologies from 1901 to 1999: a) with autocorrelation (std_c and $\delta^{13}C_c$); b) without autocorrelation (res_c and $\delta^{13}C.AR_c$).

3.3. Res_c-climate relationships

Figure 5 shows correlation and RF coefficients found between res_c and meteorological data. Non-common relationships among

Table 7. Pearson correlation coefficients between width (std_c or res_c) and δ^{13}C ($\delta^{13}C_c$ or $\delta^{13}C.AR_c$) tree-ring chronologies at each site from 1901 to 1999.

	*pn*Caz	*ps*Lil	*pu*Ped	*ps*Urb	*pu*Urb	Mean ± SD
std_c vs $\delta^{13}C_c$	0.050	−0.026	−0.183	−0.169	−0.394**	−0.144 ± 0.17
res_c vs $\delta^{13}C.AR_c$	−0.016	−0.126	−0.205[a]	−0.130	−0.274*	−0.150 ± −0.07

*p < 0.05; **p < 0.01.

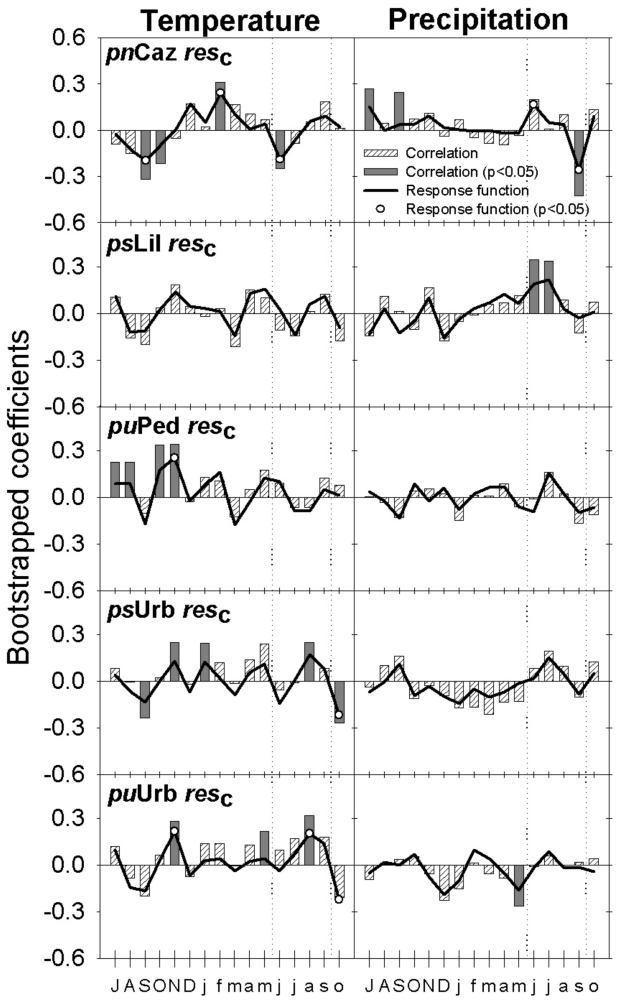

Fig. 5. Bootstrapped correlations (bars) and response functions (lines) performed between res_c and meteorological data from 1932 to 1999 (*ps*Urb and *pu*Urb) or to 2002 (*pn*Caz, *ps*Lil, *pu*Ped). Uppercase: prior year months; lowercase: current year months. Significant correlation and response function coefficients (p < 0.05) are indicated with grey bars and white circles, respectively.

the sites with their corresponding meteorological data sets were found. *Pn*Caz from southern Spain revealed significant RF coefficients with previous September (−0.195), current February (0.243) and June temperature (−0.190), as well as current June precipitation (0.165). However, the highest correlation (−0.425) and RF coefficients were found between ring-width and current September precipitation. *Ps*Lil, in the northwest, showed significant positive correlations with June and July precipitation of the current growing period (0.343 and 0.337, respectively). *Pu*Ped located in the northeast only showed significant positive correlation coefficients with temperature prior to the year of ring formation (July: 0.227; August: 0.227; October: 0.335; November: 0.343), with November also being significant in RF analysis. *Ps*Urb revealed a significant correlation with temperature of previous September (−0.238) and November (0.248), as well as with current January (0.242), August (0.247) and October (−0.271), with a significant RF coefficient only in October. Finally, *pu*Urb revealed a significant correlation with temperature of previous November (0.280), current May (0.216) and August (0.320), as well as precipitation of current May (−0.265), and also showing significant RF coefficients for temperature of previous November and current August and October.

3.4. $\delta^{13}C.AR_c$-climate relationships

Figure 6 shows correlation and RF coefficients established between the $\delta^{13}C.AR_c$ and meteorological data. During summer months, all δ^{13}C chronologies displayed significant negative correlations with summer precipitation of the current year: *pn*Caz (July: −0.362), *ps*Lil (June: −0.306; July: −0.325), *pu*Ped (June: −0.428; July: −0.472), *ps*Urb (June: −0.311; July: −0.299; August: −0.465) and *pu*Urb (July: −0.225). Accordingly, the corresponding RF coefficients were found to be significant in many cases (Fig. 6). In addition, all $\delta^{13}C.AR_c$ showed significant positive correlation coefficients with summer temperatures of the current year: *pn*Caz (September: 0.263), *ps*Lil (July: 0.243), *pu*Ped (June: 0.341; July: 0.385; August: 0.385), *ps*Urb (June: 0.212; August: 0.266) and *pu*Urb (August: 0.272). The two sites, *ps*Urb and *pu*Urb, located only 10 km away from each other, did not respond equally, showing different patterns of significance in their variables.

4. Discussion

4.1. Common variability

All trees in a stand will be affected similarly by the same set of climatically related environmental variables, as well as by

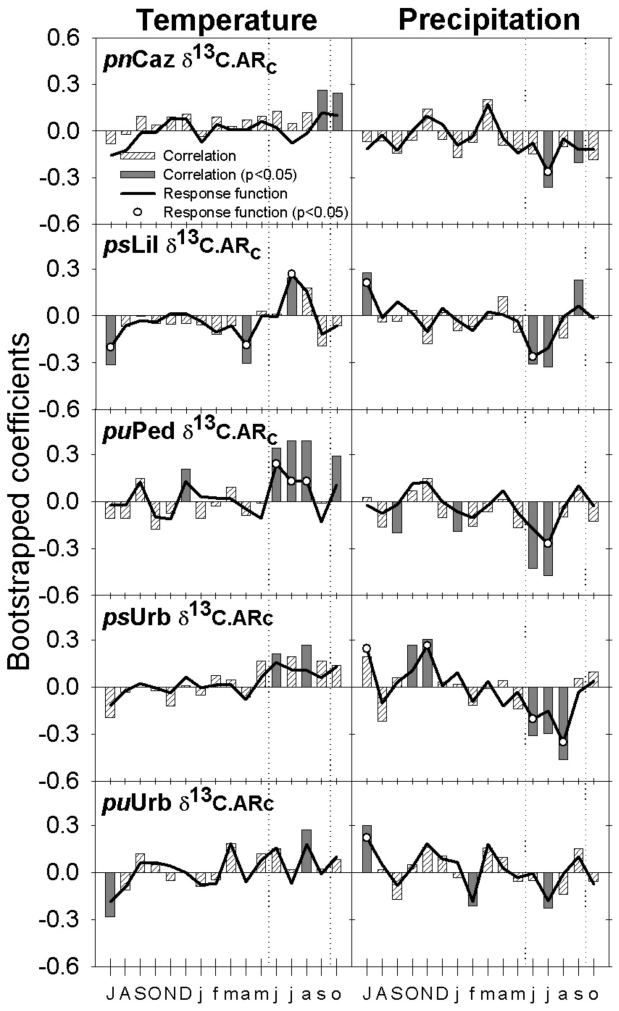

Fig. 6. Bootstrapped correlations (bars) and response functions (lines) performed between δ^{13}C.AR$_c$ and meteorological data from 1932 to 1999 (*ps*Urb and *pu*Urb) or to 2002 (*pn*Caz, *ps*Lil, *pu*Ped). Uppercase: prior year months; lowercase: current year months. Significant correlation and response function coefficients ($p < 0.05$) are indicated with grey bars and white circles, respectively.

common exogenous non-climatic factors associated with stand wide disturbances, such as fire, disease or logging (Cook, 1990). However, when similarities in growth variation are strong and spatially extensive, it is assumed that climate is related to the external agents that are forcing the observed pattern of common variability among trees, because no other environmental factors are likely to act on the same range in space, time and frequency domains (Hughes et al., 1982). Hence, on a broader scale, the common variability shared by the five chronologies across the Iberian Peninsula is most likely due to climate, as confirmed using a network of thirty-eight ring-width chronologies by Andreu et al. (2007). In a similar frequency domain, correlations among the δ^{13}C chronologies were found to be higher than between the ring-width series. Accordingly, the higher variance explained by PC1s of PCAs performed with the δ^{13}C chronologies showed that δ^{13}C variations at different sites were more similar than ring-width variations. The same finding was described by Saurer et al. (1995), who also suggested climate as the main cause of the strong similarities between δ^{13}C series from two sites. Hence, the higher and more homogenous agreement found among the carbon isotope records in comparison with ring-widths suggests that δ^{13}C ratios may better record large-scale climatic signals than ring-width variations. Furthermore, the highest correlation found between ring-width chronologies was from the sites located close to each other (*ps*Urb and *pu*Urb). In contrast, the correlation coefficient between the two δ^{13}C chronologies from the same sites was lower. This correlation coefficient was similar to coefficients found for correlations between δ^{13}C series from distant sites; therefore, our results indicate that the ring-width proxy may be more affected by local factors, whereas δ^{13}C values may contain a wider spatial climatic signal. By examining high-frequency variability, Gagen et al. (2004) found that δ^{13}C series from subalpine French Alps are less sensitive to local conditions than growth proxies (latewood width and maximum density). Studies by Robertson et al. (1997a,b) also demonstrated that significant climate signals are contained in isotopic proxies of tree-rings from Finland and England, whereas ring-widths contained little or no such information.

4.2. *Ring-width and δ^{13}C relationship*

Correlations and the PC1s revealed a negative relationship between ring-widths and δ^{13}C values (Table 7; Fig. 4). Although the interannual variability of both parameters is related to climatic variations, the same set of climate variables can lead to opposite signs, with regard to the two proxies. Warm and dry summers normally produce narrow rings (less growth), but give rise to high δ^{13}C values due to a strong reduction of the stomatal aperture for preventing unnecessary water loss. In dry conditions, discrimination against the heavier stable carbon isotope (^{13}C) during photosynthetic uptake of CO_2 is lower, leading to higher δ^{13}C values in tree-rings (Francey and Farquhar, 1982; Hemming et al., 1998). Thus, long and severe droughts generally correspond to narrow rings and less negative δ^{13}C values. However, the assessment of the climatic signal recorded in these series revealed that ring-width and δ^{13}C chronologies contain different climatic information (see sections below).

4.3. *Climatic signal and frequency domain*

The autoregressive modelling was considered by Cook et al. (1990) as a technique that removes noise or non-climatic variability from tree-ring series, when common exogenous non-climatic variance is not present in a stand. Our results highlight a higher agreement among chronologies after removing autocorrelation (due to an enhancement of the current year climatic signal), finding higher correlations among *res*$_c$ than among

std_c, as well as among $\delta^{13}C.AR_c$ than among $\delta^{13}C_c$. Robertson et al. (1997a, b) also reported that both ring-width and $\delta^{13}C_c$ indices record high-frequency common forcing better than lower-frequency forcing.

Although our chronologies showed higher similarities without autocorrelation, we did not distinguish patterns concerning which series, with or without autocorrelation, correlate better with meteorological variables, finding a wide range of responses depending on sites, frequency domain and meteorological variables. Some authors (e.g. Roberston et al., 1997a,b; Treydte et al., 2001) used the same statistical treatment for meteorological series as for tree-ring chronologies to compare the same frequency domain. However, in this work, we used raw meteorological data without applying any detrending or filtering to preserve the original temporal structure of these series. This could be one of the reasons for the heterogeneous picture found, since the highest agreement between local meteorological series and tree-ring series can be in a different frequency domain, depending on sites and kind of tree-ring proxy. Another possible explanation is that whereas common variance among chronologies is related to macroclimate, our meteorological variables represent local climate.

4.4. Climatic sensitivity of width and $\delta^{13}C$ tree-ring chronologies

Growth at the southernmost site *pn*Caz was constrained by water stress during late summer and early autumn of the preceding year, as shown by the negative relationship with previous September and October temperature and the positive correlation with previous July and September precipitation. Warm late summers can prolong the growing season, limiting the formation of metabolic reserves and consequently affecting radial growth in the following year (Fritts, 1976). Growth also showed a positive response to warm February, which might cause an early beginning of the growing season. Water stress seemed to start early at *pn*Caz, the driest site studied (see ombrotermic climate diagram in Fig. 1b), with significant response for the month of June. Similar results were reported for *P. nigra* in the southeast of Spain (Richter and Eckstein, 1991), except for the negative relationship found with September precipitation. However, Ferrio et al. (2003) found the only significant (negative) relationship for September between precipitation and radial growth in Iberian *Quercus ilex*. These results can be considered a typical ring growth response to summer droughts and rainy spring and autumn seasons under Mediterranean climatic conditions. *P. sylvestris* growth in the northwest of Spain (*ps*Lil) also seems to be sensitive to the lack of water during summer (June-July), but not to high temperatures. The influence of the Atlantic climate seems to ameliorate the growth conditions, lowering the high summer temperatures and/or lowering the atmospheric evaporative demand. Growth at the other stands did not respond to summer drought, being only sensitive to temperature. However, interesting differences exist among them. Tree-ring growth at the other *P. sylvestris* site (*ps*Urb) and at the nearby *P. uncinata* stand (*pu*Urb) was mainly limited by low temperatures (positive relationships with May and August temperatures) due to a higher continental climate influence. This influence was stronger for *pu*Urb located at a higher altitude (Table 1). Here, growth was limited by low May temperature (positive effect) in conjunction with high precipitation (negative effect) because late spring snows may delay the starting of the growing season. Finally, *P. uncinata* trees from *pu*Ped site were neither sensitive to current year precipitation nor to current year temperature. This site, located on a northeast-facing slope of the Pedraforca mountain in the pre-Pyrenees, receives ample precipitation from moist air masses evolving from the Mediterranean Sea. Nevertheless, a positive response to summer and autumn temperatures of the previous year was found. The positive response to November temperature of the preceding year shared by the two *P. uncinata* sites has also been reported in the Pyrenees (Tardif et al., 2003).

The negative response to summer rainfall detected in all $\delta^{13}C$ records showed that $\delta^{13}C$ chronologies were highly sensitive to precipitation. To a lesser degree, $\delta^{13}C$ records were also sensitive to temperature, but this response was weaker and less homogenous among sites. The differences found in the $\delta^{13}C$ response between the two nearest chronologies (*ps*Urb and *pu*Urb) may be due to species-specific and/or aspect differences of the stands and require further study.

High (less negative) $\delta^{13}C$ values reflect low concentrations of CO_2 in the intercellular air spaces of the needles, which can be due to low stomatal conductance (related to air relative humidity and antecedent rainfall) and/or high photosynthetic rates (related to temperature and photon flux) (McCarroll and Pawellek, 2001). Although the contribution of each process cannot be resolved from the current data set, the variability of $\delta^{13}C$ was probably controlled by stomatal conductance (i.e. vapour pressure deficit) at all the studied sites because of the higher sensitivity of $\delta^{13}C$ to summer precipitation than to summer temperature. Water availability appeared as a strong and consistent control variable for tree-ring $\delta^{13}C$ in all the studied stands, in agreement with the spatially broad and homogeneous common signal shared by our $\delta^{13}C$ chronologies.

Our findings are consistent with studies from other Mediterranean or semi-arid sites. Ferrio and Voltas (2005) showed that the $\delta^{13}C$ of Iberian *P. halepensis* was highly-dependent on water availability. $\delta^{13}C$ of Australian grasstrees and conifers (Swanborough et al., 2003) and $\delta^{13}C$ of Californian conifers (Feng and Epstein, 1995) were shown to be inversely correlated with rainfall, whereas studies in southwestern North America also confirm a strong influence of moisture on tree-ring $\delta^{13}C$ (Leavitt and Long, 1989; Leavitt et al., 2002). $\delta^{13}C$ of latewood cellulose from pine trees growing in dry subalpine environments in French Alps provide a powerful proxy measure of past changes in summer moisture stress, the strongest signal

being the total precipitation of July and August (Gagen et al., 2004).

In summary, each ring-width chronology investigated in this study showed its own particular relationship with climate, depending on varied stand features and local climatic conditions, whereas all the δ^{13}C chronologies shared a negative response to current year summer precipitation, as well as a positive response to current summer temperature (though the latter was less pronounced). This seems to indicate that a strong summer precipitation signal is recorded in the δ^{13}C of trees growing under Mediterranean climate, even when the mean climatic site conditions do not indicate distinct summer drought (i.e. at Pedraforca site, *pu*Ped).

Hence, δ^{13}C values reflect precipitation variability during the summer season better than tree-ring widths. This demonstrates that δ^{13}C from tree-rings can be a useful tool for assessing spatial and temporal climate variability in the Mediterranean region. δ^{13}C proxy records can fill the spatial gaps that exist between more local reconstructions from ring-width chronologies. Furthermore, δ^{13}C chronologies can provide high-quality climate reconstructions at sites where climate-growth relationships are weak.

5. Acknowledgments

We are very grateful to Oriol Bosch, Montse Ribas, Elena Muntán, Mariano Barriendos, Carlos Almarza, Pedro Antonio Tíscar, Marc Filot, Markus Leuenberger, Bruno Schull and Heinz Vos for their help during sampling, laboratory work and manuscript preparation. This research was funded by EU project ForMAT (Contract ENV4-CT97 = 0641), EU project ISONET (Contract EV K2 = 2001-00237) and EU FP6 project Millennium (GOCE 017008). The authors acknowledge the three anonymous referees for their suggestions that helped to improve the original version of the paper.

References

Andreu, L., Gutiérrez, E., Macias, M., Ribas, M., Bosch, O. and co-authors. 2007. Climate increases regional tree growth variability in Iberian pine forests. *Global Change Biol.* **13**, 804–815, doi:10.1111/j.1365–2486.2006.01322.x.

Aniol, R. W. 1983. Tree-ring analysis using CATRAS. *Dendrochronolgia* **1**, 45–53.

Biondi, F. and Waikul, K. 2004. DENDROCLIM2002: a C ++ program for statistical calibration of climate signals in tree-ring chronologies. *Comput. Geosci.-UK* **30**, 303–311.

Blanco, E., Casado, M. A., Costa, M., Escribano, R., García, M. and co-authors. 1997. *Los bosques ibéricos* (in Spanish). Editorial Planeta, Barcelona, 572 pp.

Cook, E. R. 1985. *A Time Series Analysis Approach to Tree-ring Standardization*. PhD thesis. University of Arizona, Tucson.

Cook, E. R. 1990. A conceptual linear aggregate model for tree rings. In: *Methods of Dendrochronology* (eds. E. R. Cook and L. A. Kairiukstis). Kluwer, Boston , 98–104.

Cook, E. R. and Briffa, K. R. 1990. Data Analysis. In: *Methods of Dendrochronology* (eds. E. R. Cook and L. A. Kairiukstis). Kluwer, Boston , 97–162.

Cook, E. R. and Peters, K. 1997. Calculating unbiased tree-ring indices for the study of climatic and environmental change. *Holocene* **7**, 359–368.

Cook, E. R., Briffa, K., Shigatov, S. and Mazepa, V. 1990. Tree-ring standardization and growth-trend estimation. In: *Methods of Dendrochronology* (eds. E. R. Cook and L. A. Kairiukstis). Kluwer, Boston , 104–123.

Feng, X. 1998. Long-term c_i/c_a response of trees in western North America to atmospheric CO_2 concentration derived from carbon isotope chronologies. *Oecologia* **117**, 19–25.

Feng, X. and Epstein, S. 1995. Carbon isotopes of trees from arid enviornments and implications for reconstructing atmospheric CO_2 concentration. *Geochim. Cosmochim. Acta* **59**, 2599–2608.

Ferrio, J. P. and Voltas, J. 2005. Carbon and oxygen isotope ratios in wood constituents of *Pinus halepensis* as indicators of precipitation, temperature and vapour pressure deficit. *Tellus* **57B**, 164–173.

Ferrio, J. P., Florit, A., Vega, A., Serrano, L. and Voltas, J. 2003. Δ^{13}C and tree-ring width reflect different drought responses in *Quercus ilex* and *Pinus halepensis*. *Oecologia* **137**, 512–518.

Francey, R. J. and Farquhar, G. D. 1982. An explanation of $^{13}C/^{12}C$ variations in tree-rings. *Nature* **297**, 28–31.

Fritts, H. C. 1976. *Tree Rings and Climate*. Academic Press, New York, 433 pp.

Gagen, M., McCarroll, D. and Edouard, J. -L. 2004. Latewood width, maximum density, and stable carbon isotope ratios of pine as climate indicators in a dry subalpine environment, French Alps. *Arct. Antarct. Alp. Res.* **36**, 166–171.

Gagen, M., McCarroll, D. and Edouard, J.-L. 2006. Combining ring width, density and stable carbon isotope proxies to enhance the climatic signal in tree-rings: an example from the southern French Alps. *Clim. Change* **78**, 363–379.

Guiot, J. 1991. The bootstrapped response function. *Tree-Ring Bull.* **51**, 39–41.

Helama, S., Lindholm, M., Timonen, M. and Eronen, M. 2004. Detection of climate signal in dendrochronological data analysis: a comparison of tree-ring standardization methods. *Theor. Appl. Climatol.* **79**, 239–254.

Helle, G. and Schleser, G. H. 2004. Interpreting climate proxies from tree-rings. In: *Towards a Synthesis of Holocene Proxy Data and Climate Models* (eds. H. Fischer, G. Floeser, T. Kumke, G. Lohmann, H. Miller and co-authors). Springer Verlag, Berlin, 129–148.

Helle, G., Schleser, G. H. and Bräuning, A. 2002. Climate history of the Tibetan Plateau for the last 1500 years as inferred from stable carbon isotopes in tree-rings. *IAEA CN-80/80* 301–311.

Hemming, D. L., Switsur, V. R., Waterhouse, J. S., Heaton, T. H. E. and Carter, A. H. C. 1998. Climate variation and the stable carbon isotope composition of tree ring cellulose: an intercomparison of *Quercus robur, Fagus sylvatica* and *Pinus sylvestris*. *Tellus* **50B**, 25–33.

Holmes, R. L. 1983. Computer-assisted quality control in tree-ring dating and measurement. *Tree-Ring Bull.* **43**, 68–78.

Holmes, R. L. 1992. Dendrochronology Program Library, Version 1992–1. Laboratory of Tree-Ring Research, University of Arizona, Tucson.

Hughes, M.K., Kelly, P.M., Pilcher, J.R., Lamarche, V.C. 1982. *Climate from Tree Rings*. Cambridge University Press, Cambridge, 223 pp.

IAEA 1995. TECDOC-825. Reference and intercomparison materials for stable isotopes of light elements, In: Proceedings of a Consultants Meeting , 1–3 December 1993, Vienna.

IPCC 2001. Europe (Chapter 13). In: *Climate Change 2001: Impacts, Adaptation and Vulnerability. Contribution of Working Group II to the the Third Assessment Report of the Intergovernmental Panel on Climate Change* (eds. J. J. McCarthy, O. F. Canziani, N. A. Leary, D. J. Dokken and K. S. White). Cambridge University Press, Cambridge, 643–681.

Leavitt, S. W. and Long, A. 1984. Sampling strategy for stable carbon isotope analysis of tree rings in pine. *Nature* **311**, 145–147.

Leavitt, S.W. and Long, A. 1989. Drought indicated in carbon-13/carbon-12 ratios of southwestern tree rings. *Water Resources Bull.* **25**, 341–347.

Leavitt, S.W., Wright, W.E. and Long, A. 2002. Spatial expression of ENSO, drought and summer monsoon in seasonal δ^{13}C of ponderosa pine tree rings in southern Arizona and New Mexico. *J. Geophys. Res.* **107**, 4349, doi:10.1029/2001JD001312.

Leuenberger, M. 2007. To what extent can ice core data contribute to the understanding of plant ecological developments of the past? In: *Stable Isotopes as Indicators of Ecological Change* (eds. T. Dawson and R. Siegwolf). Academic Press, London, 211–234.

Loader, N. J., Robertson, I., Barker, A. C., Switsur, V. R. and Waterhouse, J. S. 1997. An improved method for the batch processing of small wholewood samples to α-cellulose. *Chem. Geol.* **136**, 313–317.

Macias, M., Andreu, L., Bosch, O., Camarero, J. J. and Gutiérrez, E. 2006. Increasing aridity is enhancing silver fir (Abies alba Mill.) water stress in its south-western distribution limit. *Clim. Change* **79**, 289–313, doi:10.1007/s10584-006-9071-0.

Matzner, S. L., Rice, K. J. and Richards, J. H. 2001. Factors affecting the relationship between carbon isotope discrimination and transpiration efficiency in blue oak *(Quercus douglasii)*. *Aust. J. Plant Physiol.* **28**, 49–56.

McCarroll, D. and Pawellek, F. 2001. Stable carbon isotope ratios of *Pinus sylvestris* from northern Finland and the potential for extracting a climate signal from long Fennoscandian chronologies. *Holocene* **11**, 517–526.

Panek, J. A. 1996. Correlations between stable carbon-isotope abundance and hydraulic conductivity in Douglas-fir across a climate gradient in Oregon, USA. *Tree Physiol.* **16**, 747–755.

Panek, J. A. and Goldstein, A. H. 2001. Response of stomatal conductance to drought in ponderosa pine: implications for carbon and ozone uptake. *Tree Physiol.* **21**, 337–344.

Peñuelas, J., Lloret, F. and Montoya, R. 2001. Severe drought effects on Mediterranean woody flora in Spain. *For. Sci.* **47**, 214–218.

Ponton S., Dupouey, J. L., Bréda, N., Feuillat, F., Bodénès, C. and co-authors. 2001. Carbon isotope discrimination and wood anatomy variations in mixed stands of *Quercus robur* and *Quercus petraea*. *Plant Cell Environ.* **24**, 861–868.

Richter, K. and Eckstein, D. 1991. The dendrochronological signal of pine trees (*Pinus* spp.) in Spain. *Tree-Ring Bull.* **51**, 1–13.

Robertson, I., Rolfe, J., Switsur, V. R., Carter, A. H. C., Hall, M. A. and co-authors. 1997a. Signal strength and climate relationship in ^{13}C/^{12}C ratios of tree ring cellulose from oak in southwest Finland. *Geophys. Res. Lett.* **24**, 1487–1490.

Robertson, I., Switsur, V. R., Carter, A. H. C., Barker, A. C., Waterhouse, J. S. and co-authors. 1997b. Signal strength and climate relationship in ^{13}C/^{12}C ratios of tree ring cellulose from oak in east England. *J. Geophys. Res.* **102**, 19507–19516.

Saurer, M., Siegenthaler, U. and Schweingruber, F. H. 1995. The climate-carbon isotope relationship in tree rings and the significance of site conditions. *Tellus* **47B**, 320–330.

Sohn, A. W. and Reiff, F. 1942. Natriumchlorit als Aufschlussmittel (in German). *Der Papierfabrikant* **1/2**, 5–7.

Stokes, M. A. and Smiley, T. L. 1968. *An Introduction to Tree-ring Dating*. University of Chicago Press, Chicago, 73 pp.

Swanborough, P. W., Lamont, B. B. and February, E. C. 2003. δ^{13}C and water-use efficiency in Australian grasstrees and South African conifers over the last century. *Oecologia* **136**, 205–212.

Tang, K., Feng, X. and Funkhouser, G. 1999. The δ^{13}C of tree rings in full-bark and strip-bark bristlecone pine trees in the White Mountains of California. *Global Change Biol.* **5**, 33–40.

Tardif, J., Camarero, J. J., Ribas, M. and Gutiérrez, E. 2003. Spatiotemporal variability in tree growth in the central Pyrenees: climatic and site influences. *Ecol. Monogr.* **73**, 241–257.

Treydte, K., Schleser, G. H., Schweingruber, F. H. and Winiger, M. 2001. The climatic significance of δ^{13}C in subalpine spruces (Lötschental, Swiss Alps). *Tellus* **53B**, 593–611.

Wigley, T. M. L., Briffa, K. R. and Jones, P. D. 1984. On the average value of correlated time series, with applications in dendroclimatology and hydrometeorology. *J. Clim. Appl. Meterol.* **23**, 201–213.

Wilson, A. T. and Grinsted, M. J. 1977. ^{12}C/^{13}C in cellulose and lignin as palaeothermometers. *Nature* **265**, 133–135.

Yamaguchi, D. K. 1991. A simple method for cross-dating increment cores from living trees. *Can. J. For. Res.* **21**, 414–416.